AKADÉMIAI KIADÓ

UNIVERSITY of DEBRECEN

International Review of Applied Sciences and Engineering

14 (2023) 1, 76–86

DOI:
10.1556/1848.2022.00439

ORIGINAL RESEARCH PAPER

*Corresponding author.
E-mail: imaneechjijem@gmail.com

AKJournals

Effects of blade design linearization on aerodynamic performance of horizontal axis wind turbine

Imane Echjijem* and Abdelouahed Djebli

Energetic Laboratory, Sciences Faculty, Abdelmalek Essaadi University, 93030 Tetouan, Morocco

Received: December 7, 2021 • Accepted: February 24, 2022
Published online: October 5, 2022

ABSTRACT

The optimized chord and twist angle of the preliminary blade design through Blade Element Momentum theory are non-linear distributions, which adds to the complexity of blade manufacture and does not always guarantee the best aerodynamic performance. In this paper, the effect of the linearization on aerodynamic performance using Prandtl-Glauert correction model was investigated through four cases: case 1 and case 2 and case 3, where the chord and the twist angle are linearized and case 4, where sole chord is linearized. The effect of the linearization using Shen correction model while making a comparison to the linearization using Prandtl-Glauert correction model was also studied. The simulation is conducted for S809 wind turbine blade profile. The results show that case 4 using Shen correction model represents the best technique of linearization in terms of higher aerodynamic performance and easy manufacturing process.

KEYWORDS

horizontal axis wind turbine, blade element momentum theory, linearization, aerodynamic design

1. INTRODUCTION

The energy issue is at the heart of international concerns. The global economy is indeed facing a major challenge: meeting the growing need for energy while reducing greenhouse gas emissions. The use of renewable energies remains the most effective solution to this challenge. Great hope is placed in wind energy, which represents one of the world's most responsive renewable energy resources. Most wind turbines aim to capture the maximum energy from the wind. The blade is the main component that converts the kinetic energy of the wind into mechanical energy, so the design of this component has a big impact on the energy efficiency of a wind turbine. The design of a wind turbine blade is primarily based on aerodynamic modeling. In order to maximize power output and minimize costs, many researchers are trying to find methods to optimize blade design [1].

Benini and Toffolo [2] presented a bi-objective optimization method to maximize the annual energy production and minimize the energy cost for the design of a horizontal axis wind turbine. A multi-objective evolutionary algorithm and an aerodynamic model based on blade element theory were used to achieve this goal. Kale and Varma [3] have identified two main objectives to optimize the design of a wind turbine blade which are the improvement of power performance and system start-up. They showed an increase in power coefficient and a reduction in starting speed. Bottasso et al. [4] have treated an aero structural approach to optimize the design of a wind turbine blade. This approach is based on giving the profiles an appropriate position along the length of the blade according to their structural or aerodynamic role. Close to the hub zone are placed airfoils that respond to structural considerations, while in the tip zone are placed airfoils that respond to aerodynamic considerations. Mohammadi et al. [5] presented an optimization process where the goal of the work is to

maximize the output torque. This optimization is firstly performed with two variables: profile type and angle of attack; and secondly with three variables by adding the chord variable to the previous variables. They have shown that the output torque has increased very significantly when the three-variable optimization is used. Wang et al. [6] optimized the blade design of a Fixed Pitch Variable Speed wind turbine while taking into account the Reynolds number effect. The objective of this approach is to improve the energy performance of the wind turbine through optimization of the chord and twist angle for each element of the blade. Thumthae [7] sought to find optimal chord and twist angle distributions and adequate rotor speed variation to maximize the energy efficiency of a variable speed horizontal axis wind turbine.

Blade Element Momentum (BEM) theory is one of the most widely used methods in wind turbine aerodynamics as it provides an acceptable and efficient approach to wind turbine blade design and analysis [8]. However, BEM theory has failed to match the experience. To improve this theory, several studies have made corrections to this model which mainly concern the correction of tip loss. Certainly, a wind turbine with a finite number of blades is different from a wind turbine with an infinite number of blades. To account for this difference, Prandtl introduced the phenomenon of tip loss. Based on the simple one-dimensional theory that allows the prediction of the wind turbine performance, Glauert was able to develop the BEM theory. To obtain results consistent with reality, Glauert added Prandtl's tip loss correction to the calculations of the BEM theory. According to Glauert, only the induced velocities were affected by tip loss. According to de Vries, the correction includes the induced velocities as well as the mass flow. Shen et al. showed that existing tip loss corrections are not coherent and do not predict a correct physical behavior near the tip. To give better predictions of the load in the tip region, a new model for tip loss correction has been developed by Shen et al. [9, 10]. Besides, the non-linearization of the chord and twist angle of the BEM theory poses problems in the manufacturing of the wind turbine blade. Several researchers have worked on the linearization of the chord and twist angle to overcome the difficulty of manufacturing and to reduce the cost of manufacturing wind turbine blades. Manwell [11] used two constants to linearize the expression of the chord and one constant to linearize the expression of the twist angle. Maalawi et al. [12] estimated a linear distribution of the chord and an exponential distribution of the twist angle. The linearized chord is presented by a line tangential to the theoretical distribution of the chord at the blade position of 0.75*R*. Tony Burton [1] linearized the chord by drawing a straight line through the 0.75*R* and 0.9*R* positions of the theoretical chord distribution. Liu et al. [13] presented an approach to optimize the design of a fixed-pitch fixed-speed horizontal axis wind turbine blade with the objective of maximizing annual energy production and minimizing manufacturing cost. This approach is based on the linearization of the chord and twist angle distributions by both setting the chord and twist angle values at the tip of the blade and varying the values at the root of the blade. An appropriate solution is one that meets their predefined objective. Tahani et al. [14] proposed a new method of linearizing the chord and the twist angle to obtain a maximum power coefficient. Linearization consists in drawing several tangent lines at different points of the theoretical distributions of the chord and the twist angle and then selecting the line that gives a maximum power coefficient. Yang et al. [15] examined the effects of the design parameters used in linearization on the aerodynamic performance of the wind turbine blade. They also developed an optimization algorithm for linearization and an objective function that applies multiple tip speed ratios for optimizing the aerodynamic efficiency.

The BEM theory gives non-linear distributions of the optimized chord and twist angle. The non-linearization of these distributions poses problems in the manufacturing process of a wind turbine blade and does not always guarantee the best aerodynamic performance. In this paper, the effect of the linearization on aerodynamic performance using Prandtl-Glauert correction model was investigated through four cases. The effect of the linearization on the aerodynamic performance using Shen correction model was also studied. The results have determined the best technique of linearization in terms of higher aerodynamic performance and easy manufacturing process.

2. MATERIALS AND METHODS

2.1. Aerodynamic design

The aerodynamic design of a wind turbine is based on the BEM theory, which is the composition of the momentum theory and the blade element theory.

The blade element theory consists in dividing the blade into a sufficient number of elements and using the geometrical parameters of the section of the blade under study to calculate the forces acting on each of these elements [16, 17] (see Fig. 1). Therefore, the thrust dT and the torque dM given by blade element theory are as follow [18, 19]:

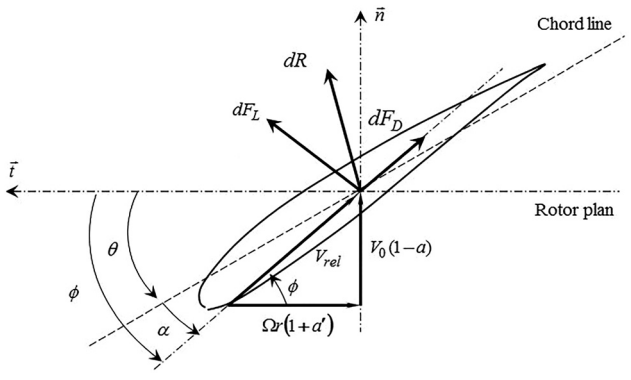

Fig. 1. Velocities and forces on a blade element

$$dT = \frac{1}{2}\rho N V_{rel}^2 c(r) C_n dr \tag{1}$$

$$dM = \frac{1}{2}\rho N V_{rel}^2 r c(r) C_t dr \tag{2}$$

where ρ is the air density, N is the number of the blade, $c(r)$ is the chord length $C_n = C_L \cos\varphi + C_D \sin\varphi$ and $C_t = C_L \sin\varphi - C_D \cos\varphi$ are the normal and tangential loads coefficients respectively, C_L and C_D are the lift and drag coefficients respectively. The relative wind speed V_{rel} and the inflow angle φ are defined as:

$$V_{rel} = V_0\sqrt{(1-a)^2 + \lambda_r^2(1+a')^2} \tag{3}$$

$$\tan\varphi = \frac{(1-a)}{\lambda_r(1+a')} \tag{4}$$

where V_0 is the wind velocity, $\lambda_r = \Omega r/V_0 = r\lambda/R$ is the local speed ratio, Ω is the angular velocity of rotor, r is the local radius, λ is the tip speed ratio, R is the radius of rotor, a and a' are the axial and the tangential induction factors respectively.

In the momentum theory, the application of axial momentum conservation and angular momentum conservation gives the thrust, torque and power coefficient expressions as follows (see Fig. 2):

$$dT = 4a(1-a)\rho V_0^2 \pi r dr \tag{5}$$

$$dM = 4a'(1-a)\rho V_0 \Omega \pi r^3 dr \tag{6}$$

$$C_P = \frac{8}{\lambda^2}\int_{\lambda_{hub}}^{\lambda} a'(1-a)\lambda_r^3 d\lambda_r \tag{7}$$

and the axial and tangential induction factors are given by:

$$a = \frac{1}{\frac{4\sin\varphi^2}{\sigma C_n} + 1} \tag{8}$$

$$a' = \frac{1}{\frac{4\sin\varphi\cos\varphi}{\sigma C_t} - 1} \tag{9}$$

where $\sigma = Bc(r)/2\pi r$ is the solidity of rotor.

However, the BEM theory is based on a rotor composed of an infinite number of blades. In fact, the rotor has a finite number of blades and the passage of air from the high pressure region to the low pressure region through the blade tips generates losses known as 'tip losses'. dT and dM are reduced due to this phenomenon which can be quantified by Prandtl's correction factor F [11]:

$$F = \frac{2}{\pi}\arccos\left[\exp\left(\frac{-N(R-r)}{2r\sin\varphi}\right)\right] \tag{10}$$

After considering tip loss factor F, the correction of dT and dM, a and a' are respectively:

$$dT = 4Fa(1-a)\,\rho V_0^2 \pi\, r dr \tag{11}$$

$$dM = 4Fa'(1-a)\,\rho V_0 \Omega\pi\, r^3 dr \tag{12}$$

$$a = \frac{1}{\frac{4F\sin\varphi^2}{\sigma C_n} + 1} \tag{13}$$

$$a' = \frac{1}{\frac{4F\sin\varphi\cos\varphi}{\sigma C_t} - 1} \tag{14}$$

Furthermore, the experimental measurements revealed that when the axial induction factor is greater than 0.5, the BEM theory is no longer valid. Therefore, several empirical models were developed [17, 20, 21] and among them we found the Spera model; For $a_c = 0.2$, the axial induction factor can be expressed as:

$$a = \begin{cases} \frac{1}{K+1} & for \quad a \le a_c \\ \frac{1}{2}\left[2 + K(1-2a_c) - \sqrt{(K(1-2a_c)+2)^2 + 4\left(Ka_c^2 - 1\right)}\right] & for \quad a > a_c \end{cases} \tag{15}$$

where $K = 4F\sin\varphi^2/\sigma C_n$.

For a real rotor, the axial velocity at the tip is not zero. Thus the angle of attack is non-zero. Using the 2D profile data gives a non-zero force near the tip, because the angle of attack is finite, this situation presents a contradiction with the correct physical behavior, where the force should tend to the zero at the tip due to pressure equalization. Therefore, it is obvious that a correction of the profile data near the tip is necessary. Shen et al. proposed to correct the lift coefficients by introducing the correction factor, F_1 as follows [9, 22]: $C_n^r = F_1 C_n$, $C_t^r = F_1 C_t$

$$F_1 = \frac{2}{\pi}\arccos\left[\exp\left(-g\frac{N(R-r)}{2r\sin\varphi}\right)\right] \tag{16}$$

$$g = \exp[-0.125(N\lambda - 21)] + 0.1 \tag{17}$$

from the momentum theory; the thrust and the torque are given by:

$$dT = 4aF(1-aF)\rho V_0^2 \pi r dr \tag{18}$$

$$dM = 4a'F(1-aF)\rho V_0 \Omega \pi r^3 dr \tag{19}$$

and from the blade element theory they are given by:

$$dT = \frac{1}{2}N\rho c(r) V_0^2 \frac{(1-a)^2}{\sin^2\varphi} C_n^r dr \tag{20}$$

$$dM = \frac{1}{2}N\rho c(r) V_0 \frac{(1-a)(1+a')}{\sin\varphi\cos\varphi}\Omega r C_t^r r dr \tag{21}$$

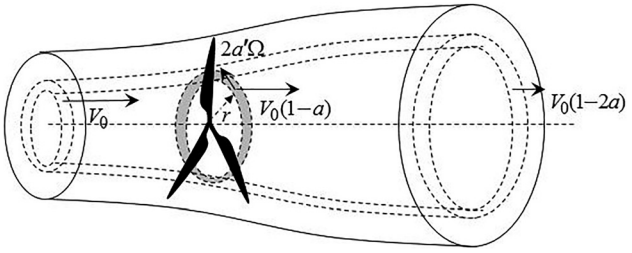

Fig. 2. One element of a multiple stream tube

then the Shen correction for induction factors:

$$a = \frac{2 + Y_1 - \sqrt{4Y_1(1-F) + Y_1^2}}{2(1 + FY_1)} \tag{22}$$

$$a' = \frac{1}{\frac{(1-aF)\ Y_2}{1-a} - 1} \tag{23}$$

where $Y_1 = 4F \sin\varphi^2/\sigma C_n^r$ and $Y_2 = 4F \sin\varphi \cos\varphi/\sigma C_t^r$.

And when a becomes greater than a critical value $a_c = 1/3$, the axial induction factor can be expressed as:

$$a = \begin{cases} \dfrac{1}{K+1} & for \quad a \le a_c \\ \dfrac{2 + Y_1 - \sqrt{4Y_1(1-F) + Y_1^2}}{2(1 + FY_1)} & for \quad a > a_c \end{cases} \tag{24}$$

where $K = 4F \sin\varphi^2/\sigma\ C_n$.

2.2. Preliminary blade design

In this paper, the optimum rotor theory [13], which takes into account the relation (25) and neglects the friction i.e. $C_D = 0$, is used to determine the chord and twist angle distributions of the preliminary blade design. The BEM theory using Prandtl-Glauert correction model is employed to calculate the aerodynamic performance of the blade. The selected profile is S809, which is considered one of the famous profiles for the design of new wind turbine blades. Figure 3 shows the lift and drag coefficients (C_l, C_d) of the profile as a function of the angle of attack at $R_e = 10^6$ [23]. The design parameters are rotor radius $R = 5.5m$, number of blade $N = 3$, wind velocity $V_0 = 7m/s$, angular velocity of rotor $\Omega = 71,93rpm$, optimal angle of attack $\alpha_{opt} = 6.16°$, optimal lift coefficient $C_{L,opt} = 0.851$, chord and twist angle distributions non-linear.

$$a' = \frac{1-3a}{4a-1} \tag{25}$$

$$c_{opt}(r) = \frac{8\pi r\left(1 - \cos\varphi_{opt}(r)\right)}{BC_{L,opt}} \tag{26}$$

$$\theta_{opt}(r) = \varphi_{opt}(r) - \alpha_{opt} \tag{27}$$

$$\varphi_{opt}(r) = \frac{2}{3}\tan^{-1}\left(\frac{1}{\lambda_r}\right) \tag{28}$$

2.3. Design linearization method

The chord and twist angle of the preliminary blade design through optimum rotor theory are non-linear distributions, which adds to the complexity of blade manufacture. The use of linear chord and twist angle distributions remains the most effective solution to avoid this complexity. On the other hand, it can also increase the aerodynamic performance. Figures 4 and 5 present the chord and twist angle distributions of the linearized blades and the preliminary blade design.

In this study, the linearization of the chord and twist angle consists first of drawing two straight lines: one passes through the positions $0.6R - 1R$ known as *linearization 1* and the other passes through the positions $0.3R - 1R$ known as *linearization 2* of the preliminary blade. It can be estimated by the following equations:

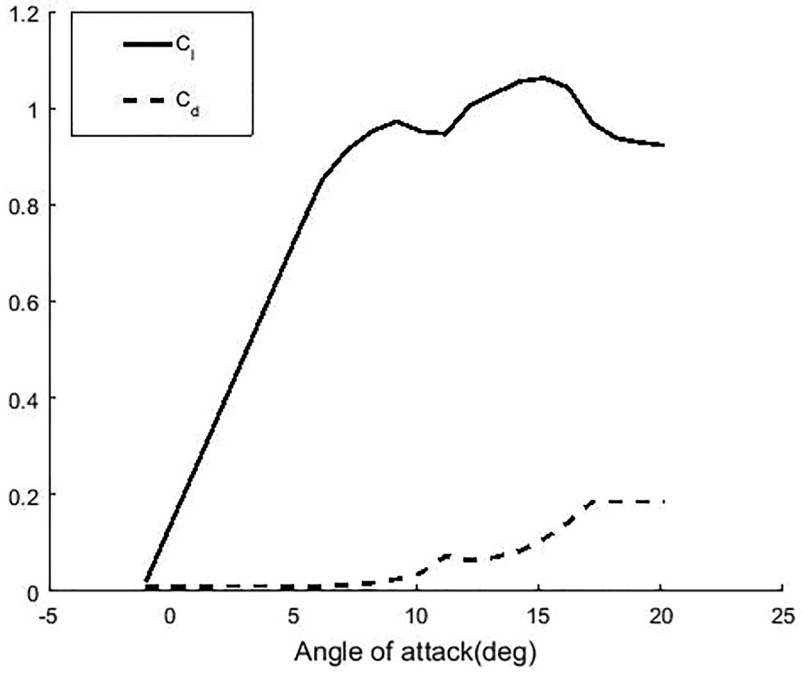

Fig. 3. Lift and drag coefficients of S809 profile

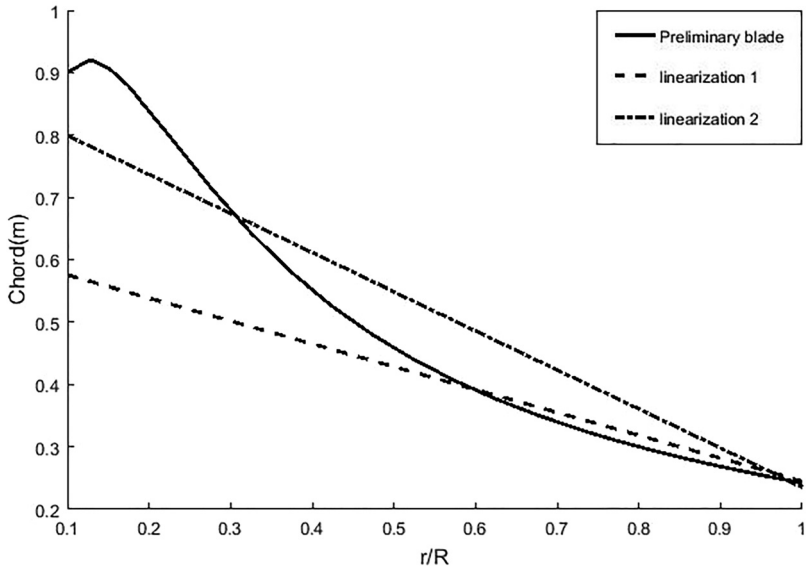

Fig. 4. Chord distribution of the linearized blades and the preliminary blade

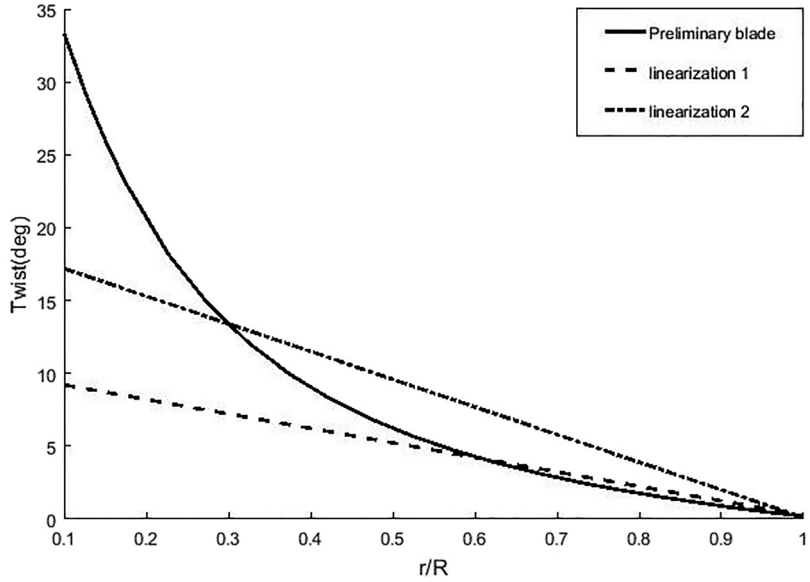

Fig. 5. Twist angle distribution of the linearized blades and the preliminary blade

$$c_{linearization\ 1} = \left[\frac{c_{1R} - c_{0.6R}}{r_{1R} - r_{0.6R}}\right](r - r_{0.1R}) + c_{0.1R} \quad (29)$$

$$\theta_{linearization\ 1} = \left[\frac{\theta_{1R} - \theta_{0.6R}}{r_{1R} - r_{0.6R}}\right](r - r_{0.1R}) + \theta_{0.1R} \quad (30)$$

$$c_{linearization\ 2} = \left[\frac{c_{1R} - c_{0.3R}}{r_{1R} - r_{0.3R}}\right](r - r_{0.1R}) + c_{0.1R} \quad (31)$$

$$\theta_{linearization\ 2} = \left[\frac{\theta_{1R} - \theta_{0.3R}}{r_{1R} - r_{0.3R}}\right](r - r_{0.1R}) + \theta_{0.1R} \quad (32)$$

where $c_{linearization\ 1}$ and $\theta_{linearization\ 1}$ are the chord and twist angle of the *linearization 1* respectively, $c_{linearization\ 2}$ and $\theta_{linearization\ 2}$ are the chord and twist angle of the *linearization 2* respectively, c_{1R}, $c_{0.6R}$, $c_{0.3R}$ and $c_{0.1R}$ are the chords at positions 1*R*, 0.6*R*, 0.3*R* and 0.1*R* of the preliminary blade respectively θ_{1R}, $\theta_{0.6R}$, $\theta_{0.3R}$ and $\theta_{0.1R}$ are the twist angles at positions 1*R*, 0.6*R*, 0.3*R* and 0.1*R* of the preliminary blade respectively. Subsequently, from *linearization 1* and *linearization 2*, four cases were extracted to be studied as follows:

Case 1 which combines $c_{linearization\ 1}$ and $\theta_{linearization\ 2}$
Case 2 which combines $c_{linearization\ 2}$ and $\theta_{linearization\ 2}$
Case 3 which combines $c_{linearization\ 1}$ and $\theta_{linearization\ 1}$
Case 4 which combines $c_{linearization\ 1}$ and $\theta_{preliminary}$ where $\theta_{preliminary}$ is twist angle of the preliminary blade.

3. RESULTS AND DISCUSSION

3.1. Linearization using Prandtl-Glauert correction model

The comparison between the thrust curves of the preliminary blade and the linearized blades is given by Fig. 6a. The latter indicates that case 1, which combines $c_{linearization\ 1}$ and $\theta_{linearization\ 2}$, and case 2, which combines $c_{linearization\ 2}$ and $\theta_{linearization\ 2}$, have smaller thrust along the blade than that of the preliminary blade design, noting that the thrust from case 1 is smaller than that of case 2. Case 3, which combines $c_{linearization\ 1}$ and $\theta_{linearization\ 1}$, decreases the thrust in the range of $0.1R - 0.75R$ and keeps it almost equal to the thrust

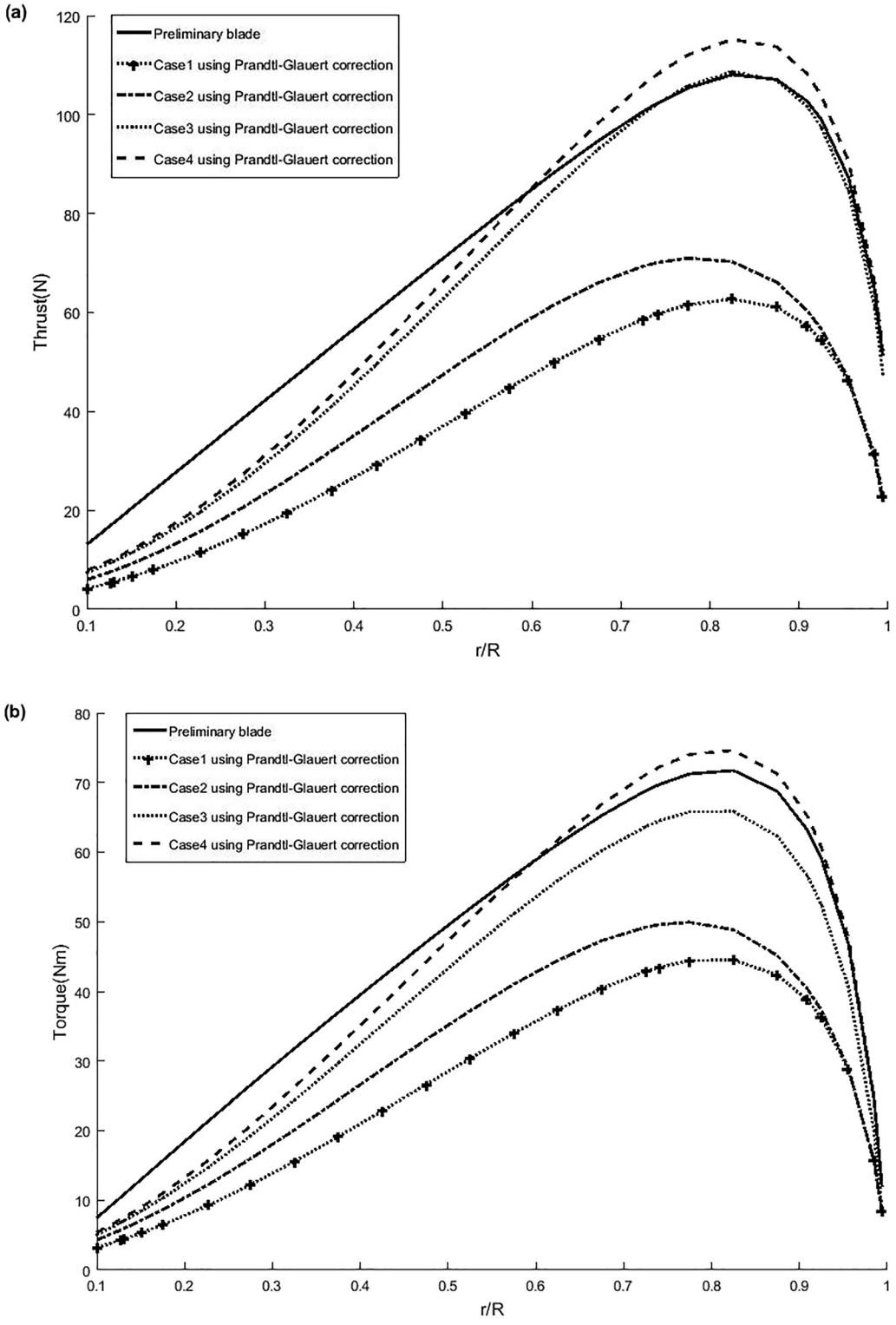

Fig. 6. Thrust and torque of the linearized blades and the preliminary blade using Prandtl-Glauert correction model

of the preliminary design in the range of $0.75R - 1R$.The thrust of case 4, which combines $c_{linearization\ 1}$ and $\theta_{preliminary}$, is higher at the positions of $0.6R$ to $1R$, and lower at the positions of $0.1R$ to $0.6R$ than that of the preliminary blade design.

The curves of the torque, the power, the power coefficient of the linearized blades, and the preliminary blade are presented in Figs 6b and 7 respectively. Compared to the preliminary blade design, case 1 and case 2 and case 3, where the chord and the twist angle are linearized, decrease the

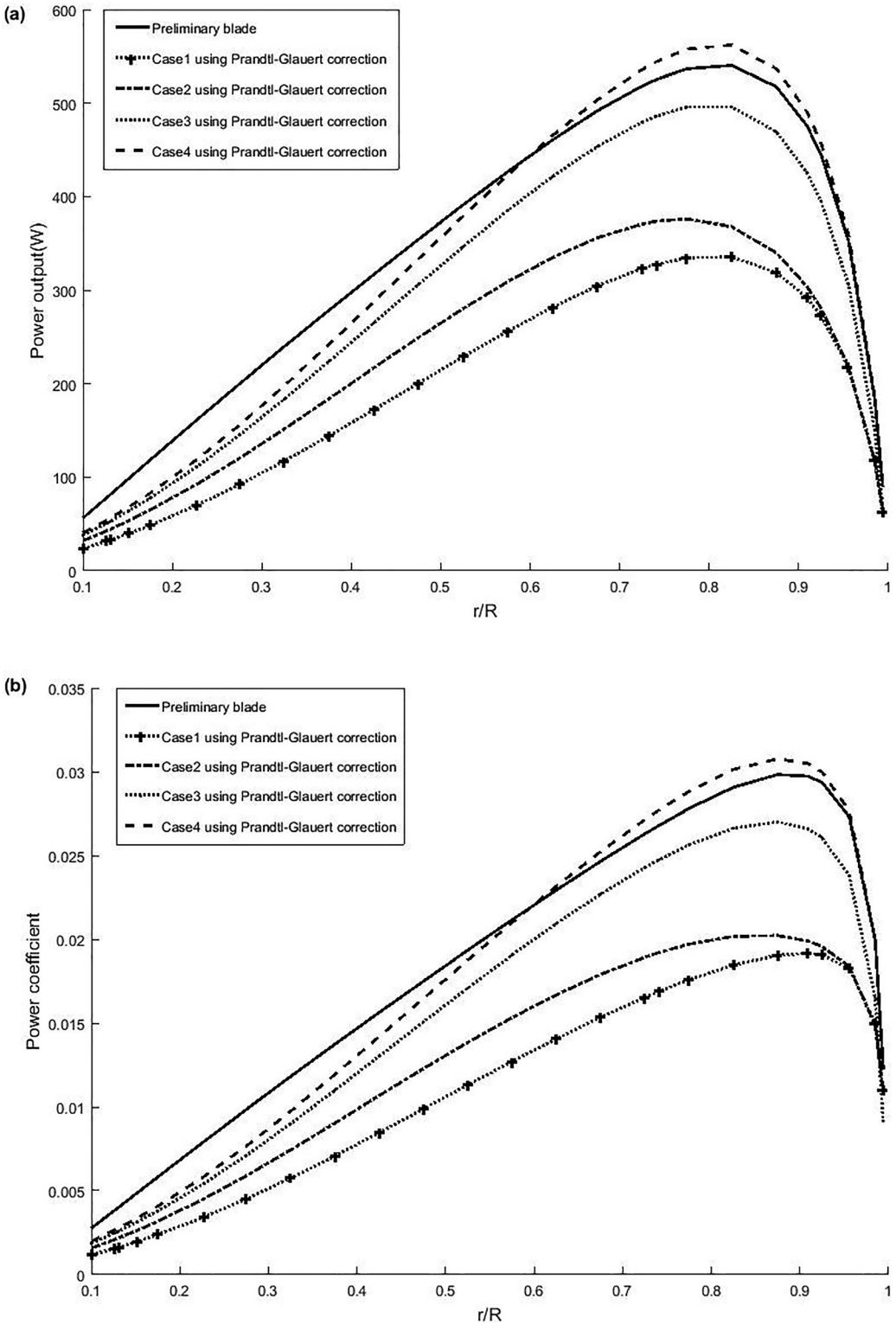

Fig. 7. Power output and power coefficient of the linearized blades and the preliminary blade using Prandtl-Glauert correction model

Table 1. Maximums of torque, power and power coefficient of linearized blades, and preliminary blade for Prandtl-Glauert correction model

		Maximum torque	Maximum power	Maximum power coefficient
Preliminary blade		71.7131	540.1787	0.0298
Linearized blades using Prandtl-Glauert correction model	Case 1	44.5459	335.5413	0.0192
	Case 2	49.9239	376.0513	0.0202
	Case 3	65.8494	496.0101	0.0270
	Case 4	74.6161	562.0450	0.0308

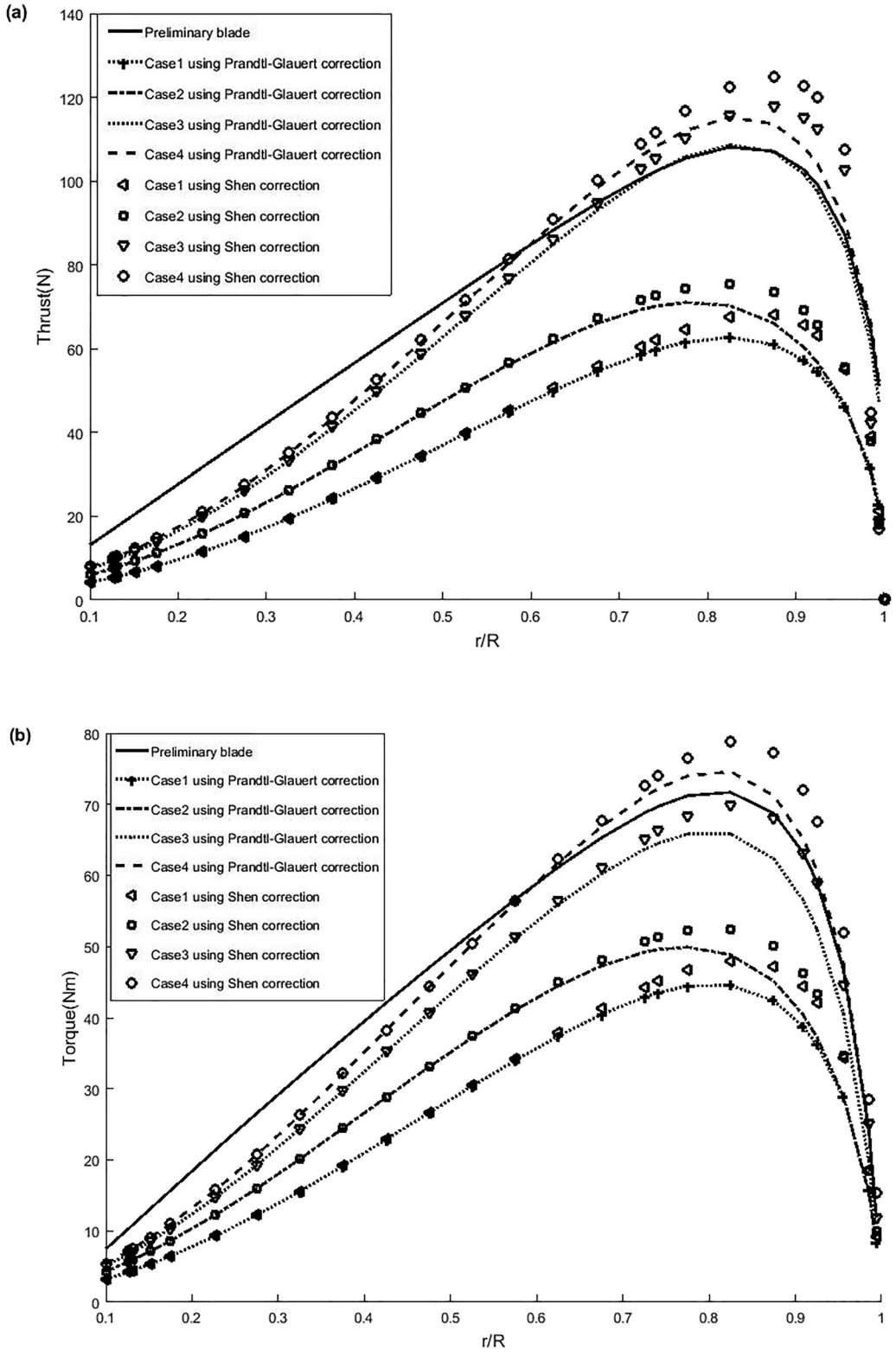

Fig. 8. Thrust and torque of the linearized blades and the preliminary blade using Shen correction model

torque, the power and the power coefficient along the blade. We see that the decrease of case 1 is more important than those of case 2 and case 3. Case 4, where sole chord is linearized at 0.6*R* and 1*R* increases the torque, the power and the power coefficient at positions from 0.6*R* to 1*R*, and decreases them at positions from 0.1*R* to 0.6*R*.

Thus, it appears that case 4 using Prandtl-Glauert correction model has the best aerodynamic performance among all four cases. Table 1 shows the maximum torque, the maximum power, and the maximum power coefficient of the linearized blades, and the preliminary blade using Prandtl-Glauert correction model. The results show that the

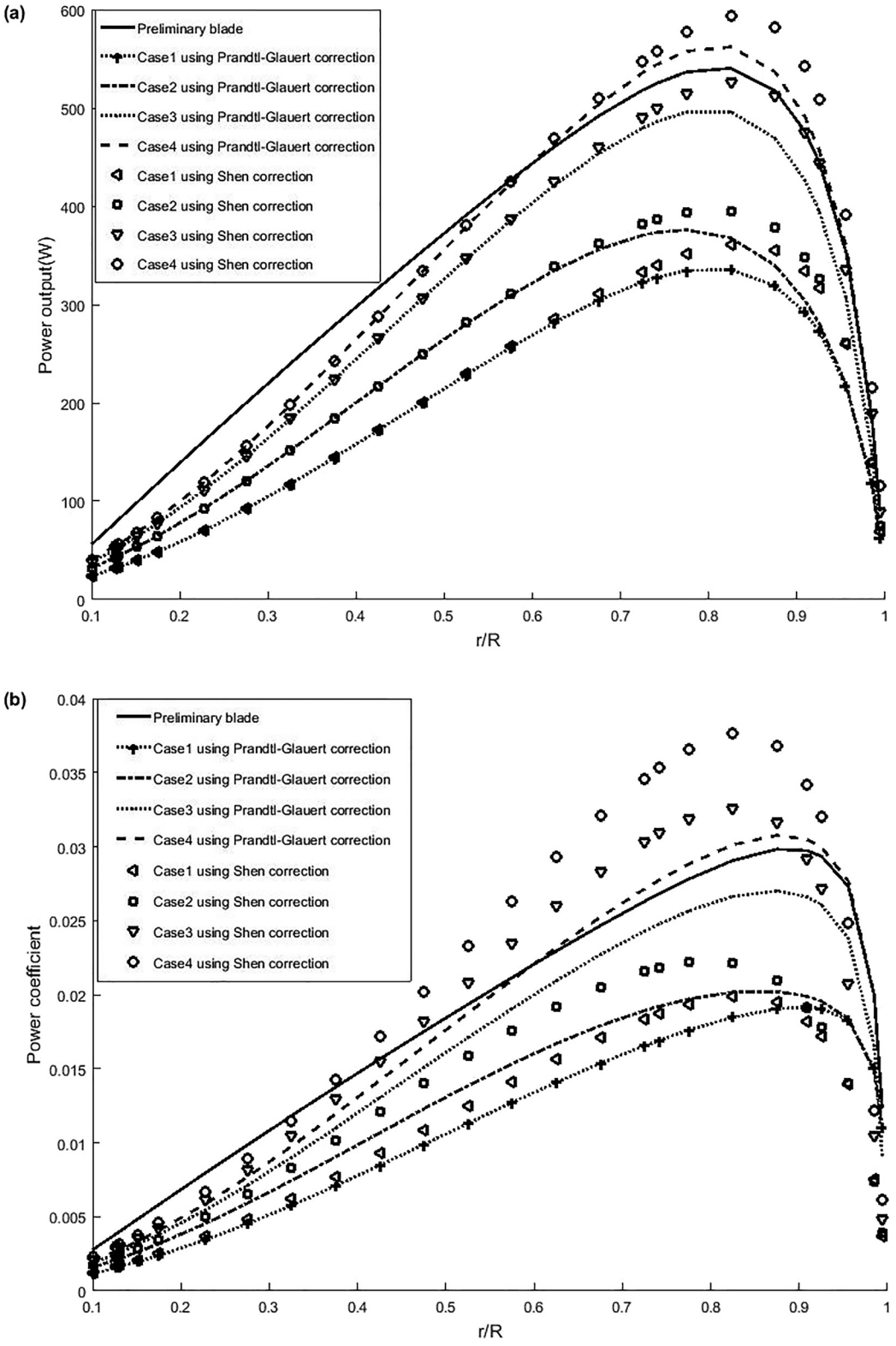

Fig. 9. Power output and power coefficient of the linearized blades and the preliminary blade using Shen correction model

Table 2. Maximums of torque, power and power coefficient of linearized blades, and preliminary blade for two correction models

		Maximum torque	Maximum power	Maximum power coefficient
Preliminary blade		71.7131	540.1787	0.0298
Linearized blades using Prandtl-Glauert correction model	Case 1	44.5459	335.5413	0.0192
	Case 2	49.9239	376.0513	0.0202
	Case 3	65.8494	496.0101	0.0270
	Case 4	74.6161	562.0450	0.0308
Linearized blades using Shen correction model	Case 1	47.9381	361.0937	0.0199
	Case 2	52.4661	395.2002	0.0222
	Case 3	69.8250	525.9560	0.0326
	Case 4	78.7702	593.3359	0.0376

single-chord linearization has a significant effect on the peak torque, power and power coefficient, which allows case 4 to increase these peaks, while the linearization of the two: chord and twist angle leads to a decrease in these peaks along the blade.

3.2. Linearization using Shen correction model

This part is interested in examining the effect of the linearization using Shen correction model on the aerodynamic performance while making a comparison to the linearization using Prandtl-Glauert correction model. There is not much difference in the root and middle of the blade between the linearization using Shen correction model and the linearization using the Prandtl-Glauert correction model in all cases (case 1, case 2, case 3, case 4) as shown in Figs 8 and 9a.

Close to the tip positions, the thrust and the torque and the power of Shen correction model are higher than using Prandtl-Glauert correction model in all cases, except for the thrust from case 3 and case 4, which is smaller than using Prandtl-Glauert correction model in the range $0.97R-1R$ of blade length. In all cases, Fig. 9b shows that near the root, the power coefficient using Shen correction model is almost equal to that using Prandtl-Glauert correction model and near to the tip positions, it is smaller than that of Prandtl-Glauert correction model. At the middle, it is higher than that of Prandtl-Glauert correction model.

Table 2 presents a comparison of the maximum torque, power and power coefficient values obtained using the Shen correction model and those obtained using the Prandtl-Glauert correction model. The result shows that in all cases, the peaks of torque, power and power coefficient increased significantly when using the Shen correction model, while maintaining case 4 as the best linearization case compared to the other cases studied.

4. CONCLUSION

The Blade Element Momentum theory gives non-linear distributions of the optimized chord and twist angle, which adds to the complexity of blade manufacture and does not always guarantee the best aerodynamic performance. To avoid this complexity and achieve easy manufacturing, we used linear chord and twist angle in the design of wind turbine blades. In this paper, the linearization of the chord and twist angle consists first of drawing two straight lines: one passes through the positions $0.6R-1R$ known as *linearization 1* and the other passes through the positions $0.3R-1R$ known as *linearization 2* of the preliminary blade. Subsequently, from *linearization 1* and *linearization 2*, four cases were extracted as follows:

Case 1 which combines $c_{linearization\ 1}$ and $\theta_{linearization\ 2}$
Case 2 which combines $c_{linearization\ 2}$ and $\theta_{linearization\ 2}$
Case 3 which combines $c_{linearization\ 1}$ and $\theta_{linearization\ 1}$
Case 4 which combines $c_{linearization\ 1}$ and $\theta_{preliminary}$ where $\theta_{preliminary}$ is twist angle of the preliminary blade.

The effect of the linearization on aerodynamic performance using Prandtl-Glauert correction model was investigated. The effect of the linearization using Shen correction model while making a comparison to the linearization using Prandtl-Glauert correction model was also studied. The results showed that case 4 using Shen correction model represents the best technique of linearization in terms of higher aerodynamic performance and easy manufacturing process.

Although the presented BEM method has advantages, it also has some limitations. In particular, we find that this method does not take into account structural considerations and cannot increase aerodynamic performance in the inner positions of the blade.

NOMENCLATURE

a	Axial induction factor
a'	Tangential induction factor
c	Chord length
N	Number of blades
C_L	Lift coefficient
C_D	Drag coefficient
V_{rel}	Relative wind speed
V_0	Wind velocity
φ	Inflow angle
θ	Twist angle
α	Angle of attack
F	Tip loss factor
r	Local radius
Ω	Angular velocity of rotor
R	Radius of rotor

ρ	Air density
λ	Tip speed ratio
λ_r	Local speed ratio
σ	Solidity of rotor
dT	Aerodynamic thrust
dM	Aerodynamic torque

REFERENCES

[1] T. Burton, N. Jenkins, D. Sharpe, and E. Bossayni, *Wind Energy Handbook*, 2nd ed. Chichester, England: John Wiley & Sons, Ltd, 2011.

[2] E. Benini and A. Toffolo, "Optimal design of horizontal-axis wind turbines using blade-element theory and evolutionary computation," *J. Sol. Energy Eng.*, vol. 124, no. 4, pp. 357–63, 2002.

[3] S. A. Kale and R. N. Varma, "Aerodynamic design of a horizontal axis micro wind turbine blade using NACA 4412 profile," *Int. J. Renew. Energy Res.*, vol. 4, no. 1, pp. 69–72, 2014.

[4] L. S. Cl Bottasso, A Croce, and F. Grasso, "Free-form design of rotor blades," *J. Phys. Conf. Ser.*, vol. 524, no. 1, 2014, Paper no. 012041.

[5] M. Mohammadi, A. Mohammadi, and S. Farahat, "A new method for horizontal axis wind turbine (HAWT) blade optimization," *Int. J. Renew. Energy Dev.*, vol. 5, no. 1, pp. 1–8, 2016.

[6] L. Wang, "Optimized chord and twist angle distributions of wind turbine blade considering reynolds number effects," *Int. Conf. Wind Energy Mater. Eng. Policies*, 2012.

[7] C. Thumthae, "Optimum blade profiles for a variable-speed wind turbine in low wind area," *Energy Proced.*, vol. 75, pp. 651–7, 2015.

[8] Y. El khchine and M. Sriti, "Improved blade element momentum theory (BEM) for predicting the aerodynamic performances of horizontal axis wind turbine blade (HAWT)," *Tech. Mech.*, vol. 38, no. 2, pp. 191–202, 2018.

[9] R. Mikkelsen, J. N. Sørensen, and W. Z. Shen, "Tip loss corrections for wind turbine computations," *Wind Energy*, vol. 8, no. 4, pp. 457–75, 2005.

[10] M. J. Clifton-Smith, "Wind turbine blade optimisation with tip loss corrections," *Wind Eng.*, vol. 33, no. 5, pp. 477–96, 2009.

[11] J. G. McGowan and J. F. Manwell, *Wind Energy Explained, Theory, Design and Application*, 2d ed. Chichester, United Kingdom: John Wiley & Sons, Ltd, 2010.

[12] K. Y. Maalawi and M. T. S. Badawy, "A direct method for evaluating performance of horizontal axis wind turbines," *Renew. Sustain. Energy Rev.*, vol. 5, no. 2, pp. 175–90, 2001.

[13] X. Liu, L. Wang, and X. Tang, "Optimized linearization of chord and twist angle profiles for fixed-pitch fixed-speed wind turbine blades," *Renew. Energy*, vol. 57, pp. 111–9, 2013.

[14] M. Tahani, G. Kavari, M. Masdari, and M. Mirhosseini, "Aerodynamic design of horizontal axis wind turbine with innovative local linearization of chord and twist distributions," *Energy*, vol. 131, pp. 78–91, 2017.

[15] K. Yang, "Geometry design optimization of a wind turbine blade considering effects on aerodynamic performance by linearization," *Energies*, vol. 13, no. 9, p. 2320, 2020.

[16] J. Pramod, *Wind Energy Engineering*. New York Chicago San Francisco: McGraw-Hill Companies, 2011.

[17] P. J. Moriarty, "AeroDyn theory manual," *Natl. Renew. Energy Lab*, 2005, no. NREL/TP-500-36881.

[18] I. Echjijem and A. Djebli, "Design and optimization of wind turbine with axial induction factor and tip loss corrections," *Proced. Manuf.*, vol. 46, pp. 708–14, 2020.

[19] Z. L. Mahri, M. S. Rouabah, and S. Zid, "Calcul des efforts aérodynamiques agissant sur les pales d'une petite éolienne," *Rev. Des Energ. Renouv.*, vol. 10, no. 2, pp. 241–56, 2007.

[20] M. L. Buhl, "A new empirical relationship between thrust coefficient and induction factor for the turbulent windmill state," *Natl. Renew. Energy Lab*, 2005, no. NREL TP-500-36834.

[21] R. Lanzafame and M. Ã. Messina, "Fluid dynamics wind turbine design: critical analysis, optimization and application of BEM theory," *Renew. Energy*, vol. 32, no. 14, pp. 2291–305, 2007.

[22] W. Xudong, W. Z. Shen, W. J. Zhu, and C. Jin, "Shape optimization of wind turbine blades," *Wind Energy*, vol. 12, no. 8, pp. 781–803, 2009.

[23] J. M. Jonkman, "Modeling of the UAE wind turbine for refinement of FAST_AD," *Natl. Renew. Energy Lab*, 2003, no. NREL/TP-500-34755.